

Specific Heat Capacity Determination by DSC

April 19, 10:00am - 11:00am EDT

Specific heat capacity (c_p) is an important, temperature-dependent material property and is often specified in material data sheets. It is a key property for improving technical processes such as injection molding, spray drying, or crystallization, as well as for the safety analysis of chemical processes and the design of chemical reactors.

Watch this session during the WAS Virtual Conference:



Dr. Jürgen Schawe

[Register Now](#)

A Transparent Membrane for Active Noise Cancellation

Philipp Rothmund, Xavier P. Morelle, Kun Jia, George M. Whitesides, and Zhigang Suo*

A method for active noise cancellation that uses an optically transparent membrane is described. The membrane consists of a prestretched hydrophobic elastomer, attached to a rigid frame and sandwiched between two hydrogels swollen with an aqueous solution of salt. The elastomer functions as a dielectric, and the hydrogel functions as an ionic conductor. When the two hydrogels are subjected to a sinusoidal voltage, the membrane generates sound. A linear model for the reflection, transmission, and generation of sound by the membrane in an impedance tube is presented and validated. Active noise cancellation is demonstrated using the linear model and feedforward control. Compared to passive sound absorption, the sound transmission loss across the membrane is improved with active control from an average value of 7 dB to an average value of 16 dB. The transparent membrane may be used to cancel noises through a window, while maintaining its transparency.

1. Introduction

Long-term exposure to loud noise—in urban life, or at work—is unpleasant and can have detrimental effects on health, even beyond the obvious damage to hearing.^[1] Passive sound insulating materials effectively attenuate noise at high frequencies, but become increasingly inefficient at lower frequencies.^[2,3] At frequencies below 500 Hz, active noise cancellation systems can be more cost effective than passive sound insulating materials, and save space.^[2]


Dr. P. Rothmund, Dr. X. P. Morelle, Prof. K. Jia, Prof. Z. Suo
John A. Paulson School of Engineering and Applied Sciences
Harvard University
29 Oxford St, Cambridge, MA 02138, USA
E-mail: suo@seas.harvard.edu

Dr. P. Rothmund, Prof. G. M. Whitesides
Department of Chemistry and Chemical Biology
Harvard University
12 Oxford St., Cambridge, MA 02138, USA

Dr. P. Rothmund, Dr. X. P. Morelle, Prof. Z. Suo
Kavli Institute for Bionano Science and Technology
Harvard University
29 Oxford Street, Cambridge, MA 02138, USA

Prof. K. Jia
State Key Laboratory for Strength and Vibration of Mechanical Structure
School of Aerospace Engineering
Xi'an Jiaotong University
Xi'an, 710049, P. R. China

Prof. G. M. Whitesides
Wyss Institute of Biologically Inspired Engineering
60 Oxford St., Cambridge, MA 02138, USA

 The ORCID identification number(s) for the author(s) of this article can be found under <https://doi.org/10.1002/adfm.201800653>.

DOI: 10.1002/adfm.201800653

An active noise cancellation system records incoming sound and generates sound that interferes destructively with it. Because destructive interference can only cancel sound locally in space, active noise cancellation is difficult to implement over the entire volume of a 3D space (e.g., a room).^[2,4] An alternative approach to sound (or noise) reduction is to inhibit the transmission of noise into a room by exciting vibrations in walls and windows.^[4] Windows are a major pathway for acoustic noise into buildings,^[5] but the development of optically transparent, active noise cancellation windows has been a challenge.^[6,7]

Here, we characterize the acoustic behavior of a transparent elastomeric membrane for active noise cancellation.

The membrane consists of a layer of a dielectric elastomer, radially stretched and clamped between two rigid dielectric rings (Figure 1a). At the center, on both faces of the dielectric, two layers of ionic conductors are attached; these ionic conductors in turn are connected via lines of ionic conductors to metallic leads fixed on the opposite sides of the rings. Because we use transparent materials for both the dielectric elastomer (VHB 4910, 3M) and the ionic conductors (a polyacrylamide hydrogel swollen with an aqueous solution of NaCl), the entire membrane is highly transparent (Figure 1b). This level of transparency is difficult to achieve with membranes sandwiched between electronic conductors, such as carbon nanotubes or silver nanowires.^[8–12]

Upon application of a voltage V to the metallic leads, ions inside the ionic conductor rearrange such that an electric field E arises across the dielectric in the region of the overlapping ionic conductors (Figure 1a). The electric field induces a Maxwell stress in the dielectric

$$\sigma = \epsilon E^2 \quad (1)$$

where ϵ is the permittivity of the elastomer.^[13,14] The Maxwell stress is equal biaxial in the plane of the membrane, and causes a reduction in thickness and an increase in area. In previous work, we used a similar setup to demonstrate a transparent loudspeaker.^[8] We applied a sinusoidal voltage to the metallic leads and the membrane generated sound over the entire audible range (20 Hz to 20 kHz), but we did not characterize the acoustic properties of the membrane in detail.

In this paper, we characterize the membrane for active noise cancellation. When an incident wave (amplitude $|F_R|$) reaches the membrane, it partially reflects (amplitude $|F_L|$), and partially transmits (amplitude $|B_R|$). The sound transmission loss (STL) across the membrane is defined by^[15]

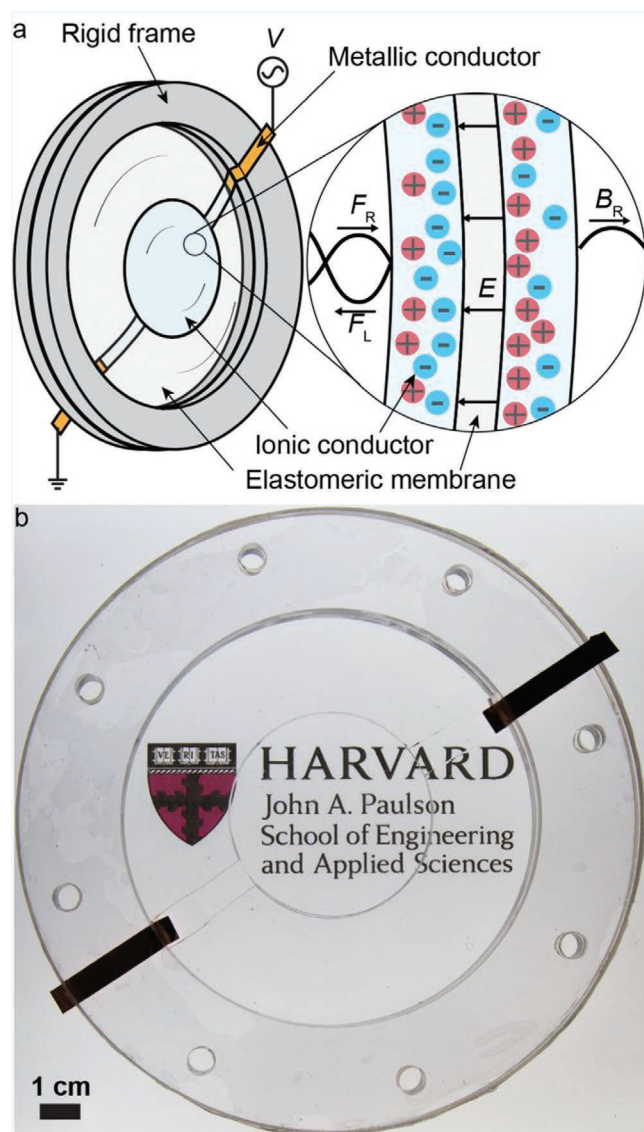


Figure 1. A transparent membrane for active noise cancellation. a) The membrane consists of a prestretched dielectric membrane clamped between two rigid circular rings. Circular, ionically conducting electrodes are attached to the center of the dielectric membrane on both faces. Thin ionic conductors connect the electrodes to metallic leads on opposite sides of the ring. An impinging acoustic sound wave (F_R) is partially reflected (F_L), and transmitted (B_R). Applying a time-dependent voltage signal (V) to the metallic conductors causes rearrangement of ions in the electrodes and leads to an electric field across the thickness of the elastomeric membrane. The resulting Maxwell stress causes oscillations of the membrane, which influence the transmitted, and reflected sound waves. b) A photograph of the transparent membrane made with an acrylic elastomer (VHB 4910 by 3M), frames of acrylic plastic, polyacrylamide hydrogels swollen with an aqueous solution of sodium chloride as ionic conductors, and conductive copper tape as metallic leads.

$$STL = 20 \log \left(\frac{|F_R|}{|B_R|} \right) \quad (2)$$

The larger the STL , the less sound is transmitted through the membrane. A goal of this paper is to investigate how to excite the membrane to increase the STL .

We propose a linear model to characterize the reflection, transmission, and generation of sound by a membrane inside an impedance tube. Although the configuration of an impedance tube differs from that of a room with a window, the idealized geometry greatly simplifies the analysis of data, and enables a basic study of the intrinsic acoustic properties of the membrane itself, rather than those of the room. We show experimentally that this linear model is valid, provided that the excitation voltage is sufficiently small. We then use the linear model to calculate the theoretical performance of active noise cancellation. All experiments are conducted in the frequency range from 150 to 1000 Hz. We demonstrate active noise cancellation with the membrane for an incident acoustic noise at an amplitude of 80 dB in a feedforward control experiment. We calculate the necessary excitation signal for the membrane with the linear model. Without an active control signal, the passive sound attenuation due to the presence of the membrane inside the impedance tube gives an average STL of 7 dB (with a peak of 19 dB). By applying an active control signal, we improve the STL to an average of 16 dB (with a peak of 37 dB).

In general, the vibration amplitude of the membrane is a nonlinear function of the excitation amplitude because i) the Maxwell stress depends on the electric field quadratically (Equation (1)), ii) the stress-strain relationship of the dielectric membrane is nonlinear, and iii) the membrane may undergo large deformation.^[16] The ability to use a linear model to describe the generation, reflection, and transmission of sound by the membrane simplifies its characterization and the control of a noise cancellation device based on this technology.

This paper demonstrates the potential of the transparent membrane in applications of active noise cancellation. The high transparency of the membrane makes it an excellent candidate for applications in which transparency is important (e.g., reduction of sound transmission through a window). Because the transparent membrane is only ≈ 2 mm thick, it will not significantly increase the volume of a window, and its planar design reduces distortion of the view through it.

Several attempts have been made to cancel noise through windows. Yu et al. used a thin film of poly(vinylidene fluoride) (PVDF) with transparent carbon-nanotube electrodes for active noise cancellation.^[6,9] The optical transmittance of the PVDF loudspeaker was 72–90% in the visible range; this loss can be noticed with the eye. Yu et al. actively reduced noise signals containing mixtures of single frequencies up to 15 dB, and they canceled random noise by ≈ 6 dB between 250 and 800 Hz. Lane excited oscillations directly in the window glass of a room with four transducers located at the edges of the window glass (which were therefore visible).^[17] He actively reduced the transmission of sound energy from a noise source with frequencies between 50 and 500 Hz, which was positioned in front of the window, into the room on average by ≈ 4 dB. Kaiser et al.^[7] and Jakob and Moser^[18] placed loudspeakers between two glass panes to excite acoustic waves in the gap between the glass panes; this design made their system bulkier than the examples described above. They actively reduced the transmission of noise at frequencies close to the resonance frequency of the double pane window by up to 18 dB.^[7]

Even though dielectric elastomers have been used as loudspeakers^[8,19–24] and proposed for active vibration suppression,^[25–27] studies of noise reduction with dielectric elastomers

have so far only been concerned with the influence of static voltages on passive sound attenuation. Lu et al. investigated the sound absorption of dielectric elastomer actuators attached to an air-filled cavity that acted as a resonator.^[28,29] Attached to the side of an impedance tube, the elastomer-cavity system reduced the sound transmission along the tube by up to 43 dB, but only at the resonance frequencies of the system. (The *STL* decreased to below 5 dB at frequencies only 25 Hz from the resonance frequencies.)^[29] By applying a constant voltage to the actuator, Lu et al. shifted the resonance frequencies and thus the absorption spectrum actively by up to 60 Hz.^[28,29] Broadband noise reduction could be achieved by combining multiple actuators with neighboring resonance frequencies.^[29] Jia et al. measured the *STL* of a flat dielectric membrane installed at the center of an impedance tube at different static voltages.^[30] They observed equally spaced *STL* peaks corresponding to the antiresonance frequencies of the membrane (i.e., frequencies at which the membrane does not oscillate), with a maximum of 15 dB at the first resonance frequency. The *STL* decreased to below 5 dB within 25 Hz from these antiresonance frequencies. By applying a static voltage to the actuator, they achieved frequency shifts of the absorption maxima by up to 65 Hz.

2. Results and Discussion

2.1. Linear Model of the Acoustic Behavior of the Transparent Membrane

We studied the acoustic properties of the transparent membrane placed in the center of an impedance tube (Figure 2). The membrane separated the tube into two sections, the front section and the back section. The tube was terminated with a coil loudspeaker at the left end, and with a foam at the right end. The impedance tube simplifies the analysis of the experimental data, because acoustic waves travel as plane waves along the axis of the tube (Figure S1, Supporting Information). Let ω be a radial frequency, which relates to the frequency f by $\omega = 2\pi f$. Let $k = \omega/c$ be the corresponding wave number, where c is the speed of sound in air. In the front section, denote the pressure of the wave traveling to the right by $F_R e^{i(\omega t - kx)}$. F_R is the complex amplitude of the wave (i.e., the magnitude $|F_R| = \sqrt{\text{Re}(F_R)^2 + \text{Im}(F_R)^2}$ is the sound pressure of the wave and the angle $\phi(F_R) = \arctan(\text{Im}(F_R)/\text{Re}(F_R))$ the phase angle of the wave). Denote the wave traveling to the left in the front section by $F_L e^{i(\omega t + kx)}$ with complex amplitude F_L . Similarly, denote the pressures of the two waves in the back section by $B_R e^{i(\omega t - kx)}$ and $B_L e^{i(\omega t + kx)}$. To determine the sound waves travelling in a section, we measured the sound pressures at two locations. The recorded signals can be decomposed into their frequency components with fast Fourier transformation. From the distance between the microphones, we can calculate the frequency spectrum of the right and left travelling waves (see Supporting Information for details).

We excited the membrane with a sinusoidal voltage of the form

$$V = V_b + V_a e^{i\omega t} \quad (3)$$

where V_b is a constant bias voltage and V_a is the amplitude of excitation. In this notation, V_a is complex valued with

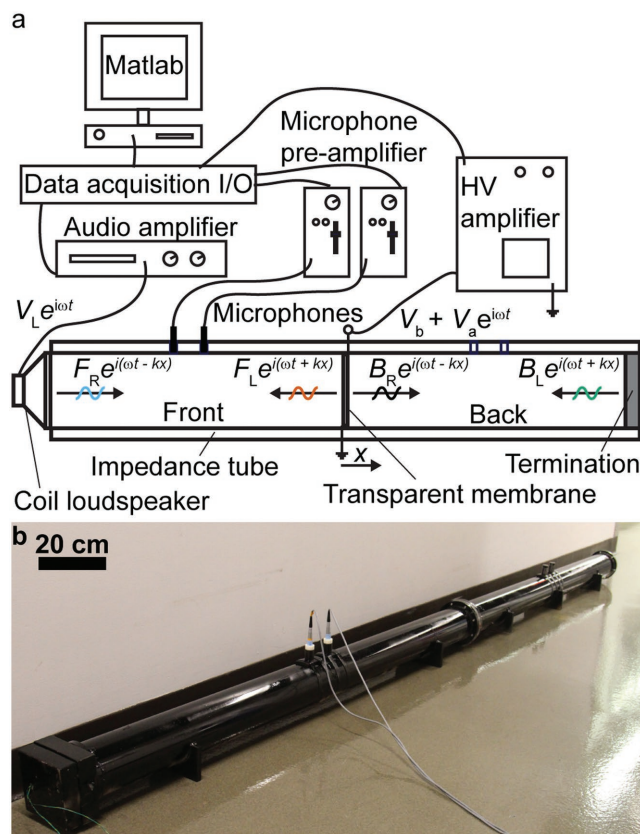


Figure 2. Schematic of the experimental apparatus. a) The transparent membrane is positioned in the center of an impedance tube, and excited through a high-voltage amplifier with a sinusoidal voltage signal of bias V_b , amplitude V_a , and radial frequency ω . A coil loudspeaker (excited with a sinusoidal voltage signal V_L through an audio amplifier) on the left end of the impedance tube acts as a noise source, whereas a foam termination at the other end reduces reflections. Sound waves travel in the front and the back sections in positive (F_R , B_R), and negative (F_L , B_L) x -direction. A pair of microphones measures sound waves in both sections. The high-voltage amplifier and the coil loudspeaker are controlled from a computer with Matlab through a data acquisition card, which also records the amplified signals from the microphones. b) Photograph of the impedance tube with the microphones installed in the front section.

the amplitude $|V_a| = \sqrt{\text{Re}(V_a)^2 + \text{Im}(V_a)^2}$, and the phase angle $\phi(V_a) = \arctan(\text{Im}(V_a)/\text{Re}(V_a))$. Due to the quadratic dependence of the Maxwell stress on the electric field (Equation (1)), the response of the membrane to the applied voltage is non-linear. When $V_b \gg |V_a|$, however, the acoustic response of the loudspeaker to the applied voltage signal is linear (as we will demonstrate here).

When the membrane is not excited, the sound waves in the front section are related to the sound waves in the back section with the transfer matrix.^[15] Under the assumption that the membrane responds linearly to small excitation amplitudes, we extended the concept of the transfer matrix by adding a term linear in the amplitude of excitation V_a :

$$\begin{pmatrix} F_R \\ F_L \end{pmatrix} = \begin{pmatrix} T_{11} & T_{12} \\ T_{21} & T_{22} \end{pmatrix} \begin{pmatrix} B_R \\ B_L \end{pmatrix} + \begin{pmatrix} S_1 \\ S_2 \end{pmatrix} V_a \quad (4)$$

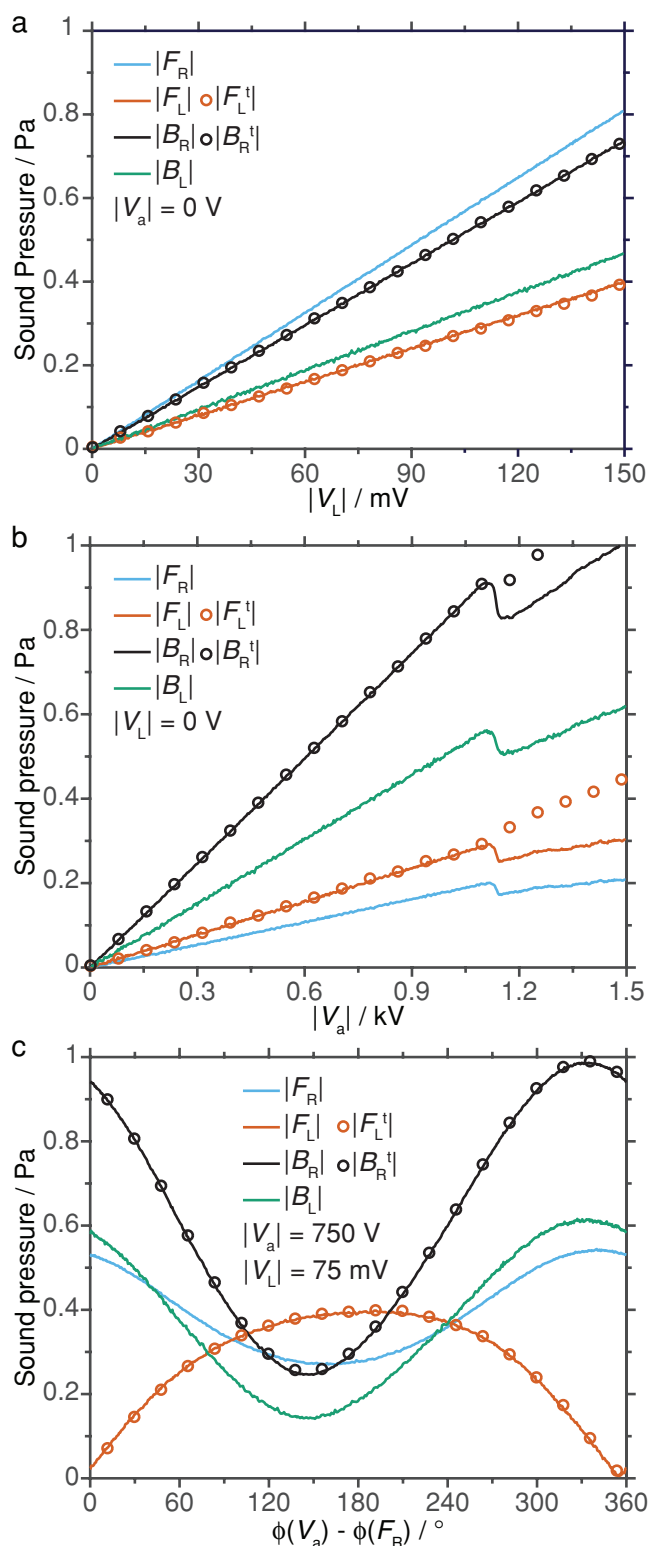


Figure 3. Comparison between theoretical model (circles), and experimental data (lines) at $f = 280$ Hz, and $V_b = 9.0$ kV. a) Fundamental components of the spectra of the sound waves for linear amplitude sweeps on the coil loudspeaker. b) Fundamental components of the spectra of the sound waves for linear amplitude sweeps on the transparent membrane. The decrease of amplitudes indicates the end of the

The components of the transfer matrix T_{ij} ($i, j = 1$, or 2) are dimensionless, and equivalent to the classical transfer matrix for passive sound attenuation (see Supporting Information for details). The excitation column S_i describes the sound generation by the membrane. All variables in Equation (4) are complex (i.e., they contain both amplitude and phase information). The matrix T_{ij} has only two independent components, because the membrane is symmetric, and we assume reciprocity.^[15] These two requirements lead to $T_{11}T_{22} - T_{12}T_{21} = 1$ and $T_{12} = -T_{21}$ (see Supporting Information for details). The parameters T_{ij} and S_i are functions of the excitation frequency f and the applied bias voltage V_b , but are independent of the lengths of the two segments, the terminations of the impedance tube, and the amplitudes of the excitation of the coil loudspeaker and the membrane.

We validated the linear model experimentally at a bias voltage of $V_b = 9.0$ kV and sinusoidal excitation signals with a (randomly chosen) frequency $f = 280$ Hz. We applied the bias voltage for 120 s before the beginning of the experiment to reduce creep effects due to viscoelasticity of the membrane.^[31] We excited the coil loudspeaker alone with a linear amplitude sweep from $V_L = 0$ mV to $V_L = 150$ mV in 60 s. We then excited the membrane alone with a 60 s long linear amplitude sweep from $V_a = 0$ kV to $V_a = 1.5$ kV. Then, we excited both the coil loudspeaker and the membrane simultaneously for 60 s with sinusoidal signals at constant amplitudes ($V_L = 75$ mV, $V_a = 750$ V), during which time we shifted the phase of the excitation signal of the membrane linearly with respect to the excitation signal of the coil loudspeaker from 0° to 360° .

When only the coil loudspeaker was excited, the amplitudes of the frequency component at $f = 280$ Hz of the four waves (obtained by short-time Fourier transformation) increased linearly with the amplitude of the voltage V_L applied to the coil loudspeaker (Figure 3a). To obtain the components of T_{ij} , we took F_R and B_L as experimentally prescribed, and fit Equation (4) to the experimental data, giving $T_{11} = 1.4 + 0.32i$, $T_{12} = -0.21 - 0.41i$, $T_{21} = 0.21 + 0.41i$, and $T_{22} = 0.76 - 0.31i$. The fitted model agrees well with the measured F_L and B_R (Figure 3a).

When we excited only the membrane, the amplitudes of the sound waves in both sections of the tube increased linearly for $V_a < 1.1$ kV (Figure 3b). At $V_a \approx 1.1$ kV, the amplitudes dropped between ≈ 0.05 and 0.1 Pa. Before this drop, the linear model agrees well with the experimental data (with T_{ij} as before, $S_1 = -0.64 + 0.38i$ Pa kV⁻¹ and $S_2 = -0.61 + 0.29i$ Pa kV⁻¹). Additionally, a subharmonic appeared in the measured acoustic spectrum at this excitation voltage (Figure S2, Supporting Information). We therefore consider the appearance of the subharmonic as an indication of the end of the frequency regime in which the linear model is valid. A reason for the end of the linear regime at $V_a \approx 1.1$ kV is the nonlinear dependence of the Maxwell stress on the excitation signal (Equation (1)). Increasing the bias voltage V_b would therefore increase maximum value of V_a for which Maxwell stress depends approximately linearly on V_a , and, thus, extend the linear regime.^[26]

linear regime. c) Fundamental components of the spectra of the sound waves for a linear phase sweep on the transparent membrane at constant excitation amplitudes plotted as a function of the difference between the phase angles of V_a and F_R .

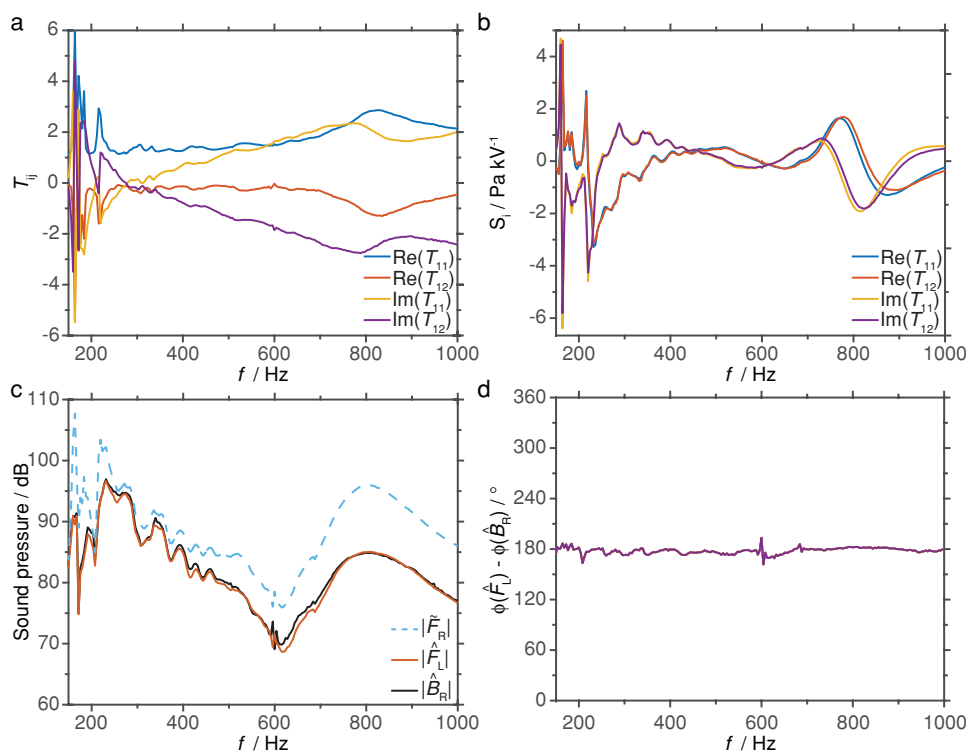


Figure 4. Characterization of the acoustic properties of the transparent membrane at bias voltage $V_b = 9.0$ kV for $150 \text{ Hz} < f < 1000 \text{ Hz}$. a) Real and imaginary components of T_{11} and T_{12} . T_{21} and T_{22} are dependent on T_{11} and T_{12} and not shown here. b) Real and imaginary components of S_1 and S_2 . c) Calculated amplitudes of the sound waves \hat{F}_L and \hat{B}_R that the membrane would emit in an impedance tube with anechoic terminations are equal because of the symmetry of the loudspeaker. The amplitude of the incident sound wave \hat{F}_R that would be completely canceled by the membrane for $|V_a| = 645 \text{ V}$. d) Because sound is generated by out of plane deformations of the membrane the phase difference between \hat{F}_L and \hat{B}_R is $\approx 180^\circ$.

When both the coil loudspeaker and the membrane were excited, the amplitudes of the acoustic waves changed with the phase difference between V_a and F_R (Figure 3c). Whereas $|F_R| / |F_L| \approx 2$, in the first part of the experiment (Figure 3a), the ratio varied in this experimental regime between $0.79 < |F_R| / |F_L| < 94$. For $|F_R| / |B_R|$ we observed similar (although not as large) changes. With the previously used values for T_{ij} and S_i , Equation (4) predicted the transmission and reflection at the membrane very well. These results demonstrate that by exciting the membrane with an appropriate amplitude and phase angle—which can be calculated with Equation (4)—one can influence sound reflection and transmission.

2.2. Characterization of the Acoustic Properties of the Transparent Membrane

We characterized the acoustic properties of the membrane (in terms of Equation (4)) in the frequency range $150 \text{ Hz} < f < 1000 \text{ Hz}$ for the bias voltage $V_b = 9.0$ kV (which we applied for 120 s before the experiment). Even though the membrane can, in principle, generate sound at frequencies below 150 Hz, we did not investigate this frequency range, because the sensitivity of the human ear to sound decreases rapidly below 150 Hz.^[32] We first applied a sinusoidal frequency sweep from 150 to 1000 Hz with a sweep rate 4 Hz s^{-1} , and amplitude of $V_L = 38 \text{ mV}$ to the coil loudspeaker. Then we excited the membrane with a sinusoidal sweep

from 150 to 1000 Hz with a sweep rate 4 Hz s^{-1} , and amplitude $V_a = 645 \text{ V}$ (at this amplitude we did not observe a subharmonic in the acoustic spectrum, Figure S3, Supporting Information). We used Equation (4) to determine the components of the transfer matrix T_{ij} (Figure 4a), and the excitation column S_i (Figure 4b) for all frequencies from the travelling waves inside the front and back sections of the tube (Figure S4, Supporting Information).

Because of resonances that depended on the length and the terminations of the impedance tube, it was difficult to judge the sound emission properties of the membrane from the raw data (Figure S4, Supporting Information). With $F_R = B_L = 0$ in Equation (4), we obtained equations for the acoustic waves \hat{F}_L and \hat{B}_R that the membrane would emit in an impedance tube with anechoic terminations on both ends (i.e., resonance effects due to the tube are removed):

$$\hat{F}_L = \left(\frac{T_{12}S_1}{T_{11}} + S_2 \right) V_a \quad (5)$$

$$\hat{B}_R = -\frac{S_1}{T_{11}} V_a \quad (6)$$

The calculated values for \hat{F}_L and \hat{B}_R ranged between 69 and 96 dB (Figure 4c) (for comparison, the noise of a street traffic at a distance of 100 ft is ≈ 70 dB, of a subway at a distance of 6 ft is ≈ 90 dB).^[33] Reducing the variation in

amplitude would require reengineering of the membrane and the frame. For all frequencies, the amplitudes of \hat{F}_L and \hat{B}_R were approximately equal. This result demonstrates that the membrane emits sound equally in both directions. This conclusion is expected from the symmetric construction of the membrane but cannot be deduced from the raw data because the terminations of the tube were asymmetric (one end was terminated by the coil loudspeaker, and the other end by the foam).

The Maxwell stress (Equation (1)) causes the reduction in the thickness of the membrane, and the expansion of its area (the in-plane mode), but the membrane can also oscillate out of plane (as does a drumhead). In our previous work we were not able to determine which mode of oscillation is predominantly responsible for sound generation.^[8] The in-plane mode generates sound waves \hat{F}_L and \hat{B}_R in phase (see Supporting Information). In the case of the out-of-plane mode, the phase difference would be 180° . The calculated phase difference of \hat{F}_L and \hat{B}_R is close to 180° (Figure 4d), which leads to the conclusion that the out-of-plane oscillation of the membrane is dominant for sound generation.

By setting $B_R = B_L = 0$ in Equation (4), we estimated the acoustic noise \tilde{F}_R that the membrane (in an ideal case) completely cancels actively, when an excitation amplitude V_a is used:

$$\tilde{F}_R = S_1 V_a \quad (7)$$

For an upper limit of the excitation voltage of $V_a = 645$ V the maximum amplitude that can theoretically completely be canceled varied with the frequency, and ranged between $|\tilde{F}_R| = 76$ dB (\approx sound of an automobile at 20 ft distance)^[33] and 107 dB (\approx sound of motorcycle at 20 ft distance)^[33] (Figure 4c). It is possible to increase the linear regime and, thus, the maximum canceled noise amplitude, by increasing the bias voltage V_b .

2.3. Passive Noise Attenuation versus Active Noise Cancellation

By setting $B_L = V_a = 0$ in Equation (4), we obtained an equation for the sound transmission loss due to passive attenuation STL_p^a by the membrane for an impedance tube with anechoic termination:^[15]

$$STL_p^a = 20 \log(|T_{11}|) \quad (8)$$

We observed strong resonance peaks in STL_p^a for frequencies between 150 and 250 Hz, with amplitudes up to 19 dB (Figure 5). The frequencies, at which the resonance peaks occur, can be modified by changing the bias voltage. Increasing V_b lowers the frequencies of the resonance peaks, whereas decreasing V_b shifts the resonance peaks to higher frequencies.^[30] STL_p^a was 3–12 dB, without clear resonance peaks, in the range of frequencies from 250 to 1000 Hz. Jia et al. reported the same behavior for a dielectric elastomer actuator with electrodes made of carbon grease.^[30]

To illustrate active noise cancellation (at $V_b = 9.0$ kV) based on the linear model, we actively canceled an acoustic sound wave that consisted of a sinusoidal frequency sweep (sweep rate 4 Hz s^{-1}) from 150 to 1000 Hz, with amplitude

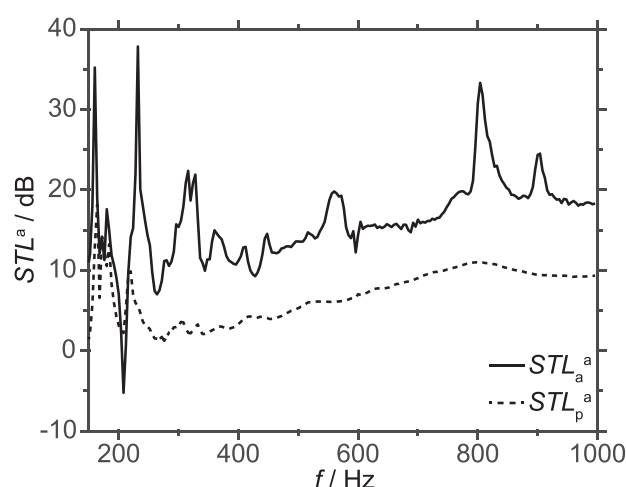


Figure 5. Comparison of the sound transmission loss of passive sound attenuation (STL_p^a) and active noise cancellation (STL_a^a) for an incident sound wave $|F_R| = 80$ dB in an impedance tube with anechoic termination calculated using the linear model and the experimental results. Except for close to 200 Hz, the active sound cancellation outperforms passive sound attenuation.

$|F_R| \approx 80$ dB (sound of a light truck at 20 ft distance)^[33] with feedforward control. We calculated the necessary excitation signal (Figure S5, Supporting Information) with Equation (7), using the previously determined value for S_1 (Figure 4b). To avoid the nonlinear regime, we limited the excitation amplitude to 645 V. As mentioned above, the incident sound wave F_R is composed of the sound wave generated by the coil loudspeaker and of the reflection of F_L at the coil loudspeaker and was therefore also influenced by the excitation signal of the membrane. Exploiting the linearity of the coil loudspeaker, we adjusted its excitation voltage during the sweep to keep the amplitude and phase of F_R approximately constant (Figure S5, Supporting Information).

We derived an equation analogous to Equation (8), which corrects the sound transmission loss for resonance effects of the tube by subtracting the influence of the reflected wave B_L :

$$STL_a^a = 20 \log \left(\left| \frac{\hat{F}_R}{\hat{B}_R} \right| \right) = 20 \log \left(\left| \frac{|F_R|}{B_R + \frac{T_{12}}{T_{11}} B_L} \right| \right) \quad (9)$$

We used the recorded pressure waves (Figure S6, Supporting Information), the previously determined values of T_{ij} (Figure 4a), and Equation (9) to calculate the sound transmission loss STL_a^a for an anechoic tube during active noise cancellation (Figure 5). Also see Figure S7 in the Supporting Information for a comparison of STL_a^a to the uncorrected sound transmission loss based on Equation (2). Except for the region close to 200 Hz, active noise cancellation outperformed passive attenuation. The sound transmission loss increased from an average of 7 dB with a peak of 19 dB for passive sound attenuation, to an average of 16 dB with a peak of 37 dB for active noise cancellation.

3. Conclusion

This paper establishes that sound transmission and reflection at the membrane can be actively controlled by an applied voltage. The linear response to sinusoidal excitation voltages at small amplitudes allows relatively simple control. With simple active feedforward control based on the linear model developed here we could increase the average *STL* through the membrane (compared to passive sound attenuation) by $\approx 100\%$ (i.e., we reduced the average transmitted sound amplitude by a factor of ≈ 3 compared to passive sound attenuation).

Compared to the work by Yu et al., the transparent membrane in this work achieves a similar sound transmission loss, but has higher optical transmittance ($>99\%$, as opposed to $72\text{--}90\%$).^[6,8,9] The improvement of the sound transmission loss obtained with active control in this paper exceeds the one reported by Lane.^[17] It is comparable to the one achieved by Kaiser et al., but the membrane used here requires less space ($\approx 2\text{ mm}$ as opposed to $\approx 8\text{ cm}$).^[7]

Testing the acoustic behavior of the membrane in an impedance tube simplified the sound field to plane waves. Further work is required to test the performance of the membrane under more realistic conditions. This work would include not only more complex acoustic waves (e.g., nonplanar acoustic field, moving source of noise), but also interactions of the membrane with close structures (e.g., the influence of the interspace, when attached to a window).^[29]

The membrane provides a new method for active noise cancelation for applications in which space is limited and high optical transparency is required. Examples include windows, wall panels, and protective gear in loud workplaces. The design of the membrane is not limited to a planar, circular shape with a rigid frame. Nonplanar, deformable membranes may enable unusual, adaptable acoustic properties, such as directionality of the emitted sound.

4. Experimental Section

Fabrication of the Ionic Conductor: A salt-containing hydrogel as a stretchable, transparent, ionic conductor was used.^[8] To synthesize the hydrogel, the following substances purchased from Sigma Aldrich were used: Acrylamide (AAm, monomer), ammonium persulfate (APS, initiator), *N,N,N',N'*-tetramethylethylenediamine (TEMED, accelerator), *N,N'*-methylenebis(acrylamide) (MBAAm, crosslinker), and sodium chloride (NaCl). The polyacrylamide (PAAm) hydrogel was synthesized using the following protocol. AAm (47.3 g) in deionized water (300 mL) was dissolved to form an aqueous monomer solution (2.22 M), to which MBAAm (293 mg), TEMED (162 mg), and APS (87 mg) were added. After degassing the prepared solution, it was poured into a glass mold ($120 \times 80 \times 1\text{ mm}^3$), which was covered with a glass plate. The sample was kept at room temperature for 24 h to allow the polyacrylamide network to form, and then it was soaked for at least 2 days in an aqueous NaCl solution (2.75 M).

The ionic conductor was cut with a laser cutter (VersaLaser VLS 3.5) into a paddle like shape (Figure 1b). The diameter of the circular center was 51 mm, the width of the lead 7.5 mm, and the length of the lead 25 mm.

Fabrication of the Transparent Membrane: To fabricate the transparent membrane (Figure 1), VHB 4910 (3M) was used as dielectric elastomer. Two layers of VHB 4910 (3M) were stuck together, stretched biaxially to three times their initial dimension, and clamped them between two acrylic rings (inner diameter 4 in, outer diameter 6 in). On opposite sides of

the frame, copper tapes (0.5 cm wide) were attached. On each face of the dielectric membrane, a hydrogel electrode was attached, so that their circular regions overlapped in the center, and the thin ionic leads connected to the copper tapes. To improve adhesion between the hydrogels and the dielectric elastomers, the surfaces of the hydrogels were dried with a stream of N_2 before attaching them to the elastomers. The adhesion energy was low ($\approx 0.5\text{ J m}^{-2}$), but was adequate for the experiments.^[34]

The Impedance Tube: All experiments were performed inside a custom-made impedance tube (Figure 2). Similar impedance tubes have been widely used to measure the sound transmission loss of acoustic materials.^[4,15,35,36] The impedance tube (cut-off frequency $\approx 2\text{ kHz}$) consisted of two 5 ft-long sections of PVC tubing (inner diameter 4 in, outer diameter 5 in). One-inch thick flanges were glued to the ends of the tubes to attach the coil loudspeaker (GUI Inc., GF1004), the membrane and a termination (2 in thick polyurethane foam). The transparent membrane was positioned in the center of the impedance tube. The sound waves were measured at the centers of the front and the back sections of the impedance tube with a pair of microphones (Bruel & Kjaer, 4192-L-001) with preamplifiers (Listen Inc., SoundConnect), which were spaced 8 cm apart. The transparent membrane was excited through a high-voltage amplifier (Trek 30/20A), and the coil loudspeaker with a commercial audio-amplifier (AudioSource, AMP100VS). Signal generation and recording were done with Matlab through a DAQ-card (National Instruments, USB-6218).

Every experiment was performed twice. In the first experiment, the acoustic pressure was recorded in the front section. For the second experiment, the microphones were moved to the back section of the tube. The openings of the section without microphones were covered with plugs. From the frequency components of the recorded signals (obtained by short time Fourier transformation), the amplitudes and phases of the acoustic waves were calculated in the two sections of the impedance tube (see Supporting Information).

Supporting Information

Supporting Information is available from the Wiley Online Library or from the author.

Acknowledgements

This work was supported by NSF MRSEC (DMR 14-20570). X.P.M. was supported by the Cabeaux-Jacobs BAEF fellowship for one year at Harvard University.

Conflict of Interest

The authors declare no conflict of interest.

Keywords

acoustics, active noise cancelation, dielectric elastomer actuators, hydrogels, ionic conductors

Received: January 25, 2018

Revised: April 18, 2018

Published online: May 22, 2018

[1] W. Passchier-Vermeer, W. F. Passchier, *Environ. Health Perspect.* **2000**, *108*, 123.

[2] C. H. Hansen, *Understanding Active Noise Cancellation*, Spon Press, London **2001**.

- [3] Z. Yang, H. M. Dai, N. H. Chan, G. C. Ma, P. Sheng, *Appl. Phys. Lett.* **2010**, 96, 41906.
- [4] H. Zhu, R. Rajamani, K. A. Stelson, in *Proc. of the 2002 American Control Conf.*, Vol. 2, IEEE, New York **2002**, p. 909.
- [5] Y. Shen, D. J. Oldham, *J. Sound Vib.* **1982**, 84, 11.
- [6] X. Yu, R. Rajamani, K. A. Stelson, T. Cui, in *Proc. of the 2006 American Control Conf.*, IEEE, New York **2006**, p. 704.
- [7] O. E. Kaiser, S. J. Pietrzko, M. Morari, *J. Sound Vib.* **2003**, 263, 775.
- [8] C. Keplinger, J.-Y. Sun, C. C. Foo, P. Rothmund, G. M. Whitesides, *Z. Suo, Science* **2013**, 341, 984.
- [9] X. Yu, R. Rajamani, K. A. Stelson, T. Cui, *Sensors Actuators* **2006**, 132, 626.
- [10] Z. Yu, Q. Zhang, L. Li, Q. Chen, X. Niu, J. Liu, Q. Pei, *Adv. Mater.* **2006**, 23, 664.
- [11] D. McCoul, W. Hu, M. Gao, V. Mehta, Q. Pei, *Adv. Electron. Mater.* **2016**, 2, 1500407.
- [12] V. Scardaci, R. Coull, J. N. Coleman, *Appl. Phys. Lett.* **2010**, 97, 23114.
- [13] R. Pelrine, R. Kornbluh, Q. Pei, J. Joseph, *Science* **2000**, 287, 836.
- [14] Z. Suo, *Acta Mech. Solida Sin.* **2010**, 23, 549.
- [15] ASTM E2611-09, *Standard Test Method for Measurement of Normal Incidence Sound Transmission of Acoustical Materials Based on the Transfer Matrix Method.*, ASTM International, West Conshohocken, PA, USA **2009**.
- [16] Z. Suo, X. Zhao, W. H. Greene, *J. Mech. Phys. Solids* **2008**, 56, 467.
- [17] J. Lane, *Master Thesis*, University of Canterbury, Christchurch, New Zealand **2013**.
- [18] A. Jakob, M. Möser, *Appl. Acoust.* **2003**, 64, 163.
- [19] R. Heydt, R. Kornbluh, J. Eckerle, P. Pelrine, in *Proc. SPIE 6168* (Ed: Y. Bar-Cohen), SPIE, San Diego, CA, USA **2006**, 61681M.
- [20] R. Heydt, R. Pelrine, J. Joseph, J. Eckerle, R. Kornbluh, *J. Acoust. Soc. Am.* **2000**, 107, 833.
- [21] A. J. Moustgaard, R. W. Jones, B. Lassen, R. Sarban, in *Proc. of the ASME Conf. on Smart Materials, Adaptive Structures and Intelligent Systems*, vol. 1, Amer Soc Mechanical Engineers, New York **2010**, 63.
- [22] K. Hochradel, S. J. Rupitsch, A. Sutor, R. Lerch, D. K. Vu, P. Steinmann, *Appl. Phys. A* **2012**, 107, 531.
- [23] T. Sugimoto, A. Akio, K. Ono, Y. Morita, K. Hosoda, D. Ishii, K. Nakamura, *J. Acoust. Soc. Am.* **2013**, 134, EL432.
- [24] N. Hosoya, S. Baba, S. Maeda, *J. Acoust. Soc. Am.* **2015**, 138, EL424.
- [25] R. Sarban, R. W. Jones, *J. Intell. Mater. Syst. Struct.* **2012**, 23, 473.
- [26] J. Zhu, S. Cai, Z. Suo, *Int. J. Solids Struct.* **2010**, 47, 3254.
- [27] J. Zhu, S. Cai, Z. Suo, *Polym. Int.* **2010**, 59, 378.
- [28] Z. Lu, Y. Cui, J. Zhu, Z. Zhao, M. Debiassi, *J. Acoust. Soc. Am.* **2013**, 134, 4218.
- [29] Z. Lu, Y. Cui, J. Zhu, M. Debiassi, in *Proc. SPIE 9056* (ed. Y. Bar-cohen), SPIE, Sand Diego, Ca, USA, **2014**, 90562N.
- [30] K. Jia, M. Wang, T. Lu, J. Zhang, T. Wang, *Smart Mater. Struct.* **2016**, 25, 55047.
- [31] C. C. Foo, S. Cai, S. J. A. Koh, S. Bauer, Z. Suo, *J. Appl. Phys.* **2012**, 111, 34102.
- [32] ISO 226:2003, *Acoustics — Normal equal-loudness-level contours*, International Organization for Standardization, Geneva, Switzerland **2003**.
- [33] S. K. Argarwal, *Noise Pollution*, APH Publishing Corporation, New Delhi, India **2009**.
- [34] J. Tang, J. Li, J. J. Vlassak, Z. Suo, *Soft Matter* **2016**, 12, 1093.
- [35] J. Y. Chung, D. A. Blaser, *J. Acoust. Soc. Am.* **1980**, 68, 907.
- [36] J. Y. Chung, D. A. Blaser, *J. Acoust. Soc. Am.* **1980**, 68, 914.